

rAAV-delivered PTEN therapeutics for prostate cancer

Jianzhong Ai,^{1,2} Jia Li,² Qin Su,² Hong Ma,² Qiang Wei,¹ Hong Li,¹ and Guangping Gao²

¹Department of Urology, Institute of Urology, West China Hospital, Sichuan University, 88 South Keyuan Road, Chengdu 610041, China; ²Horae Gene Therapy Center, University of Massachusetts Medical School, 368 Plantation Street, Worcester, MA 01605, USA

Effective treatments for prostate cancer (PCa) require further development, and previous studies have reported that PTEN and its downstream target CDKN1B are significantly downregulated in PCa cells compared with normal cells. Therefore, modulation of PTEN and CDKN1B expression might be a promising therapeutic approach for PCa treatment. Expression of PTEN and CDKN1B was verified in specimens from PCa patients and transgenic adenocarcinoma mouse prostate (TRAMP) mice. The effect of PTEN on PCa cell migration, apoptosis, and the cell cycle was analyzed *in vitro* using a wound-healing assay and flow cytometry. We assessed the ability of intraprostatic and intratumoral injections of recombinant adeno-associated virus (rAAV) 9 expressing Pten or Cdkn1b into TRAMP mice and a subcutaneous tumor xenograft mouse model, respectively, to inhibit PCa progression. PTEN and CDKN1B were significantly downregulated in human and mouse PCa samples, and CDKN1B expression correlated positively with PTEN expression. PTEN overexpression significantly inhibited cell migration and cell-cycle progression and promoted apoptosis in PCa cells by decreasing Ccnd1 expression and increasing that of Cdkn1b. Importantly, treatment with the rAAV9.Pten or rAAV9.Cdkn1b extended the lifespan of TRAMP mice and inhibited the growth rate of tumor xenografts by regulating downstream gene expression. Moreover, neoplasia in treated prostates was significantly diminished compared with that in control prostates, and apoptosis was markedly observed in xenografts treated with Pten or Cdkn1b. These data indicate that rAAV-based PTEN/CDKN1B delivery is promising for the development of novel therapeutics for PCa.

INTRODUCTION

Prostate cancer (PCa) is the second most commonly diagnosed cancer and the second leading cause of cancer-related deaths among men in 46 countries.¹ Drugs for different targets have been developed for the treatment of PCa, including sipuleucel-T,² abiraterone,³ enzalutamide,⁴ and docetaxel.⁵ However, tumor cell growth and metastasis are not completely inhibited by these therapeutics, and PCa relapse is a major challenge for the effective treatment of PCa. In recent decades, many studies have investigated the underlying mechanism involved in the occurrence and development of PCa, and many innovative drug candidates have been provided,^{6,7} though the efficacies of

these drugs need to be improved. Androgen receptor (AR) signaling plays a crucial role in PCa progression, and drugs targeting this pathway cause significant PCa suppression;⁸ nevertheless, off-target effects are induced by mutation, alternative splicing, or ligand mismatching of these targets. Therefore, novel therapeutics should be developed for effective PCa treatment based on different perspectives.

Phosphatase and tensin homolog (PTEN) is a well-known tumor-suppressor gene involved in many types of carcinomas, including PCa,⁹ liver cancer,¹⁰ breast cancer,¹¹ lung cancer,¹² and colorectal cancer.¹³ Specifically, in patients with androgen-dependent PCa (ADPC) and castration-resistant PCa (CRPC), one copy of the PTEN gene has often been lost.¹⁴ PTEN loss causes an increase in PIP3 cellular content and ultimately promotes AKT activity and its downstream function.⁹ Therefore, PTEN is deemed an important negative regulator of PI3K/AKT signaling that plays important roles in cancer. PI3K inhibitors have been developed to inhibit tumor progression; however, their clinical applications have been hampered by serious side effects and toxicity.⁹ As a critical modulator of PI3K/AKT signaling, therapeutics that target PTEN warrant investigation.

Interestingly, Li et al. reported that CDKN1B and CCND1, two downstream genes of PTEN, exhibit copy-number alteration (CNA) deletions and amplification, respectively, in PCa.¹⁵ Furthermore, as a cyclin-dependent kinase inhibitor, CDKN1B has been shown to be a reliable prognostic marker for PCa; hence, low expression of CDKN1B is correlated with a poor prognosis.¹⁶ PTEN enhances CDKN1B expression levels by activating its transcription and reducing its degradation.¹⁷ Moreover, the expression and nuclear localization of CCND1 is negatively regulated by PTEN, and PTEN orchestrates cell proliferation by synergistically regulating CCND1 and CDKN1B.¹⁷ These findings imply that PTEN signaling exerts a pivotal effect on tumor cell proliferation by regulating cell-cycle arrest; thus, PTEN might be an ideal

Received 28 December 2020; accepted 28 November 2021;
<https://doi.org/10.1016/j.omtn.2021.11.018>.

Correspondence: Jianzhong Ai, Department of Urology, Institute of Urology, West China Hospital, Sichuan University, 88 South Keyuan Road, Chengdu 610041, China.

E-mail: jianzhong.ai@wchscu.cn

Correspondence: Guangping Gao, Horae Gene Therapy Center, University of Massachusetts Medical School, 368 Plantation Street, Worcester, MA 01605, USA.

E-mail: guangping.gao@umassmed.edu



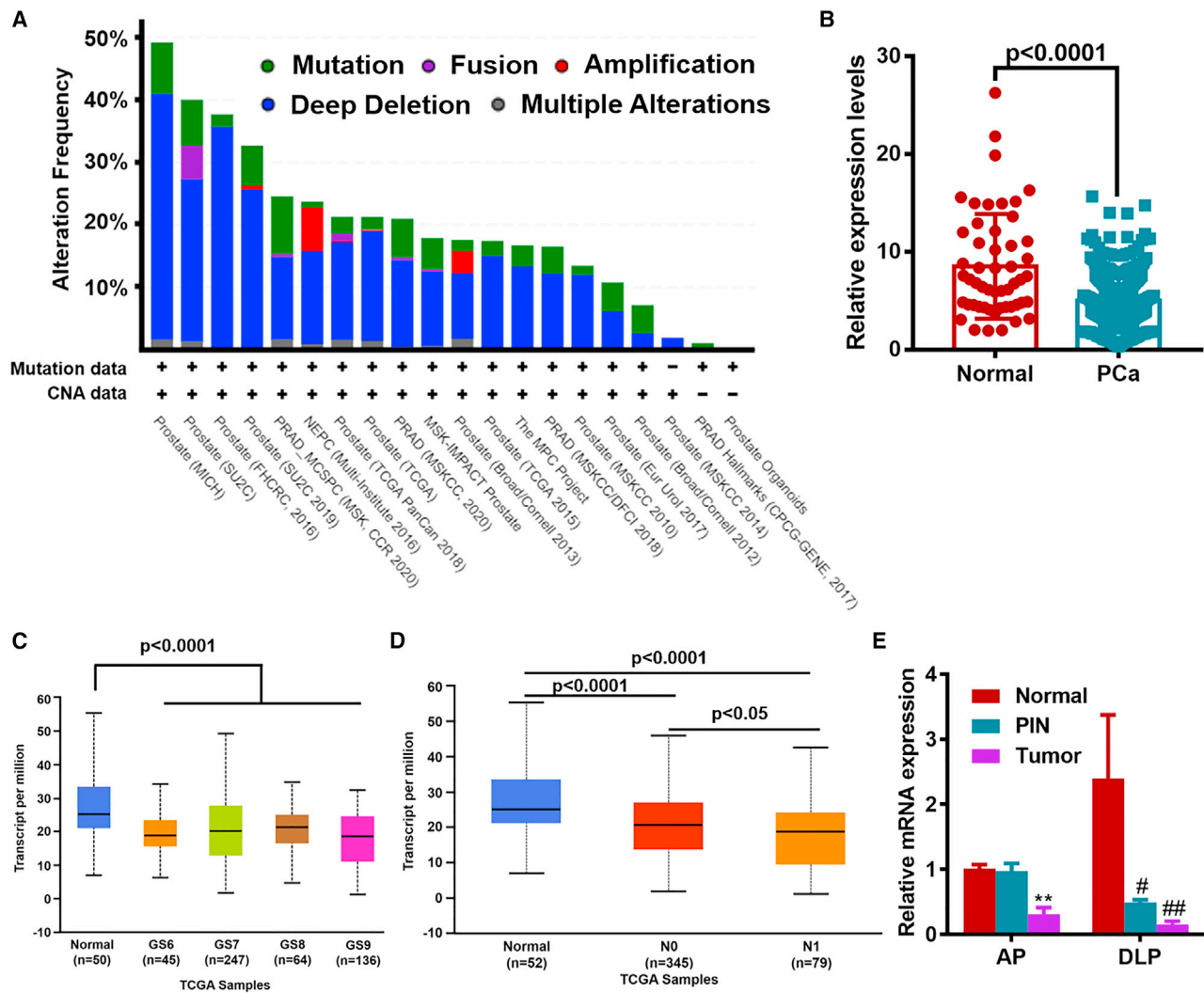


Figure 1. PTEN expression pattern in human and mouse PCa

(A) The panels showing PTEN gene alteration frequency demonstrate that PTEN gene deletion and mutation are two common events reported in various studies. (B) Data from TCGA indicated significant downregulation. (C) PTEN expression in the normal and PCa groups with different Gleason scores. (D) PTEN expression in the normal and PCa groups with different degrees of lymph node metastasis. (E) PTEN expression was obviously decreased with PCa progression. CNA, copy-number alteration; GS, Gleason score; AP, anterior prostate; DLP, dorsal lateral prostate. **p < 0.01 compared with normal AP; #p < 0.05 and ##p < 0.01 compared with normal DLP.

therapeutic target to inhibit PCa progression. However, the delivery of therapeutic genes into the normal prostate or PCa cells is still an immense challenge.

Our previous studies showed that recombinant adeno-associated virus (rAAV) can effectively and safely transduce normal prostate tissue and PCa cells, making it a powerful tool for developing novel therapeutics for PCa.^{18,19} Compared with other viral vectors, rAAVs possess many advantages for gene delivery, i.e., long-term gene expression, high transduction efficiency, wide tissue tropism, and low immunogenicity.^{18,20} Watanabe et al. utilized AAV serotype 2 to deliver Maspin into PCa xenografts, which led to a significant suppression of tumor growth.²¹

In this study, we first investigated the role of PTEN in inhibiting PCa progression, and second, we explored the therapeutic effects of rAAV-based gene delivery *in vivo* using a transgenic mouse model and a xenograft model. The findings provide an important foundation for the clinical application of rAAV-based gene therapy for PCa, which would be greatly beneficial for these patients.

RESULTS

Downregulation of PTEN in human and mouse PCa specimens

To determine the expression pattern of PTEN in PCa tissues, we first analyzed its alteration frequency using The Cancer Genome Atlas (TCGA) data from cBioPortal. As shown in Figure 1A, deep deletion of and mutations in PTEN were common in PCa samples. Thus,

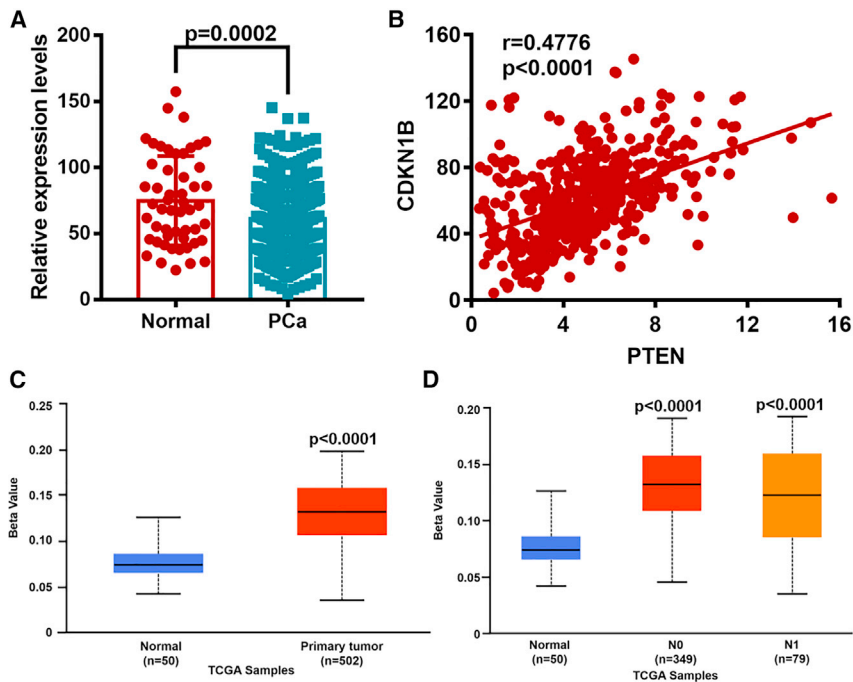


Figure 2. CDKN1B expression in human PCa

(A) TCGA data analysis showed a marked reduction in CDKN1B in PCa samples compared with control samples. (B) Correlation analysis of the expression of PTEN and CDKN1B. (C and D) The methylation levels of the CDKN1B gene promoter were evaluated between the normal and PCa groups.

PTEN expression was significantly downregulated in PCa samples, and its expression was unrelated to the Gleason score (Figures 1B and 1C). Interestingly, PTEN expression was negatively correlated with lymph node metastasis (Figure 1D). In the transgenic adenocarcinoma mouse prostate (TRAMP) mouse model, Pten downregulation was accompanied by PCa progression (Figure 1E).

Decreased expression of CDKN1B in PCa samples

By mining TCGA data, we found that CDKN1B expression was markedly reduced in PCa samples (Figure 2A) and that its expression was positively correlated with PTEN expression ($r = 0.4776$) (Figure 2B). Intriguingly, an obviously high methylation level was detected at the promoter region of CDKN1B in PCa tissue, and this level was not affected by the status of lymph node metastasis (Figures 2C and 2D), which might be one reason for the reduction in CDKN1B expression since a high methylation level can inhibit gene transcription.

PTEN overexpression significantly inhibits PCa cell migration and cell-cycle progression and promotes cell apoptosis

To further study the role of PTEN in regulating PCa progression, PTEN was overexpressed in the PCa cell line PC3, the migration of which was assessed using a wound-healing assay. As shown in Figures 3A–3C, the mRNA and protein levels of PTEN were dramatically upregulated in PC3 cells. Moreover, the wound width in the PTEN overexpression group was significantly greater than that in the mock group (Figures 3D and 3E). Next, apoptosis and the cell-cycle status of PC3 cells were evaluated using flow cytometry. PTEN overexpression markedly promoted PC3 cell apoptosis (Figures 4A and 4B); nevertheless, the cell cycle was inhibited signifi-

cantly by PTEN (Figures 4C and 4D). Moreover, cell proliferation was assessed by Cell Counting Kit-8 (CCK-8) assay, and the data indicated that PTEN obviously decreased PC3 cell proliferation (Figure 4E). To reveal the underlying mechanism, the expression of two important genes downstream of PTEN, CCND1, and CDKN1B was assayed, and the results showed that PTEN overexpression markedly decreased CCND1 and increased CDKN1B expression (Figure 4F). Furthermore, PTEN or CDKN1B overexpression also promoted the apoptosis and inhibited the cell cycle of C42B-MDV cells, a cell line expressing AR with enzalutamide resistance (Figure S1). These findings indicated that PTEN can inhibit PCa cell migration and the cell cycle and can promote apoptosis, at least in part, by regulating CCND1 and CDKN1B expression.

Pten and Cdkn1b suppress PCa progression in a TRAMP model

To elucidate the therapeutic roles of Pten and Cdkn1b, rAAV9.Pten or rAAV9.Cdkn1b was intraprostatically injected into the mouse prostate, and the DNA and mRNA levels were detected in the anterior prostate (AP) and dorsal lateral prostate (DLP). As shown in Figure 5, the DNA and mRNA levels of Pten and Cdkn1b were significantly elevated in the AP and DLP. Furthermore, the transduction pattern of rAAV9 in the prostate was evaluated using EGFP as a reporter gene, and our previous findings indicated that prostate epithelial cells could be efficiently transduced by rAAV9.²² Additionally, the body weights of the mice in the three groups were not markedly different (Figure 6A). Importantly, the survival status of mice in the Pten and Cdkn1b groups was obviously improved, and the median survival of mice in the mock, Pten, and Cdkn1b groups was 220, 301, and 365 days, respectively (Figure 6B). Furthermore, hematoxylin and eosin (H&E) staining showed that neoplasia in the AP and DLP in mice in the Cdkn1b and Pten groups was diminished compared with that in mice in the mock group (Figure 6C). Importantly, Pten overexpression markedly promoted the expression of its downstream gene Cdkn1b at both the mRNA and protein levels (Figures 7A, 7B, and 7C) and altered the phosphorylation level of Cttnb1, another target of Pten (Figures 7B and 7C). However, the mRNA and protein expression of Ccnd1 was dramatically decreased by Pten (Figures 7A, 7B, and 7C). These results were consistent with those in previous studies, which also showed that the regulation of gene expression by Pten can explain its role in the inhibition of PCa progression. These

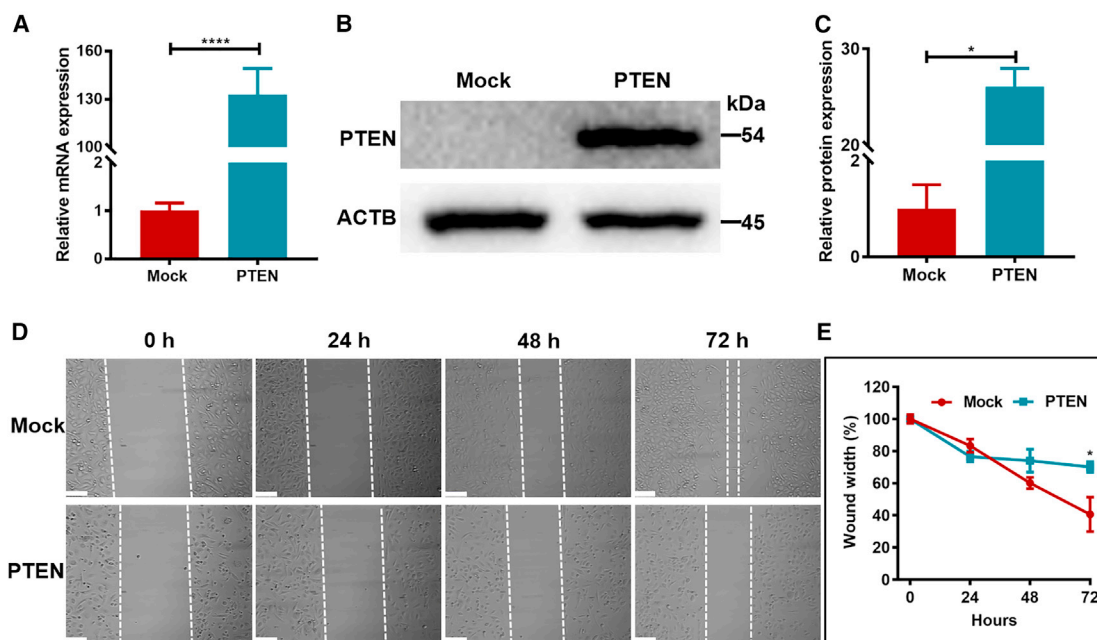


Figure 3. PTEN overexpression significantly inhibits PCa migration *in vitro*

(A) qPCR detection of PTEN mRNA levels. (B) The protein level of PTEN was detected in PC3 cells. (C) The intensities of the protein bands were determined using ImageJ software. (D) A wound-healing assay was used to assess the migration ability of PC3 cells, and representative images are shown. (E) Real-time measurement of the width of the wound showed that PTEN overexpression markedly decreased PC3 cell migration. The experiments were performed in triplicate, and three replicates were included in each group. * $p < 0.05$; **** $p < 0.0001$.

findings suggest that Pten and Cdkn1b can effectively inhibit PCa development by modulating the expression of downstream genes.

Pten and Cdkn1b repress tumor growth in an immunocompetent xenograft mouse model by increasing apoptosis

To confirm the inhibitory role of Pten and Cdkn1b in PCa progression, a xenograft model in which TRAMP-C2 cells were injected into C57/B6 mice was established; the rAAV plasmids were then intratumorally injected when the tumor volume reached approximately 100 mm^3 (Figure 8A). As illustrated in Figure 8B, the tumor growth rates of mice in the Pten and Cdkn1b groups were significantly lower than those of the mock group, and the expression of Pten and Cdkn1b in tumor tissues was also markedly increased (Figures 8C and 8D). H&E staining of tumor tissue did not show obvious pathological differences among these three groups; however, the apoptosis rate of tumor cells in the Pten and Cdkn1b groups was significantly increased compared with that in the mock group (Figure 8E). These findings indicated that Pten and Cdkn1b can effectively inhibit tumor growth and might be ideal targets for PCa treatment.

DISCUSSION

PCa is a disease that threatens the survival and quality of life of patients with this cancer. Overall, the mortality rate of PCa is increasing, even with early surveillance based on prostate-specific antigen (PSA) detection.²³ ADPC can be effectively treated with androgen deprivation therapy (ADT). However, tumor cells can

become resistant to this type of treatment due to genomic reprogramming or other causes, whereby ADPC evolves toward CRPC. In CRPC, AR mutation, overexpression, and alternative splicing occur in tumor cells, and the effect of AR signaling on tumor cell growth is significantly diminished.²⁴ Furthermore, androgen can be released from tumor cells themselves or from the adrenal glands.²⁵ Based on this understanding, novel endocrine therapeutics have been developed that decrease androgen synthesis and the binding between androgen and AR. Abiraterone is a CYP17 inhibitor, which is crucial for androgen synthesis in the testes, adrenal glands, and tumor cells.²⁶ After ADT treatment, tumor cells are more sensitive to low levels of androgen; hence, this is an alternative for effective PCa treatment that completely blocks androgen synthesis. Moreover, as AR activity in tumor cells is promoted by binding androgen, agents blocking the binding of AR and androgen may have an inhibitory effect on PCa progression. Enzalutamide was designed to competitively bind AR, and thus, tumor cell growth can be inhibited by repressing the activity of AR signaling.²⁷ In general, both abiraterone and enzalutamide were designed to target the AR signaling axis, and efficacies for PCa inhibition at the early stage are promising. Nonetheless, these inhibitory effects can be reduced and even disappear after several months of treatment.²⁸

Therefore, the underlying mechanisms of resistance and relapse require further exploration, and a breakthrough for effective treatment of PCa could be achieved from this perspective. PTEN and

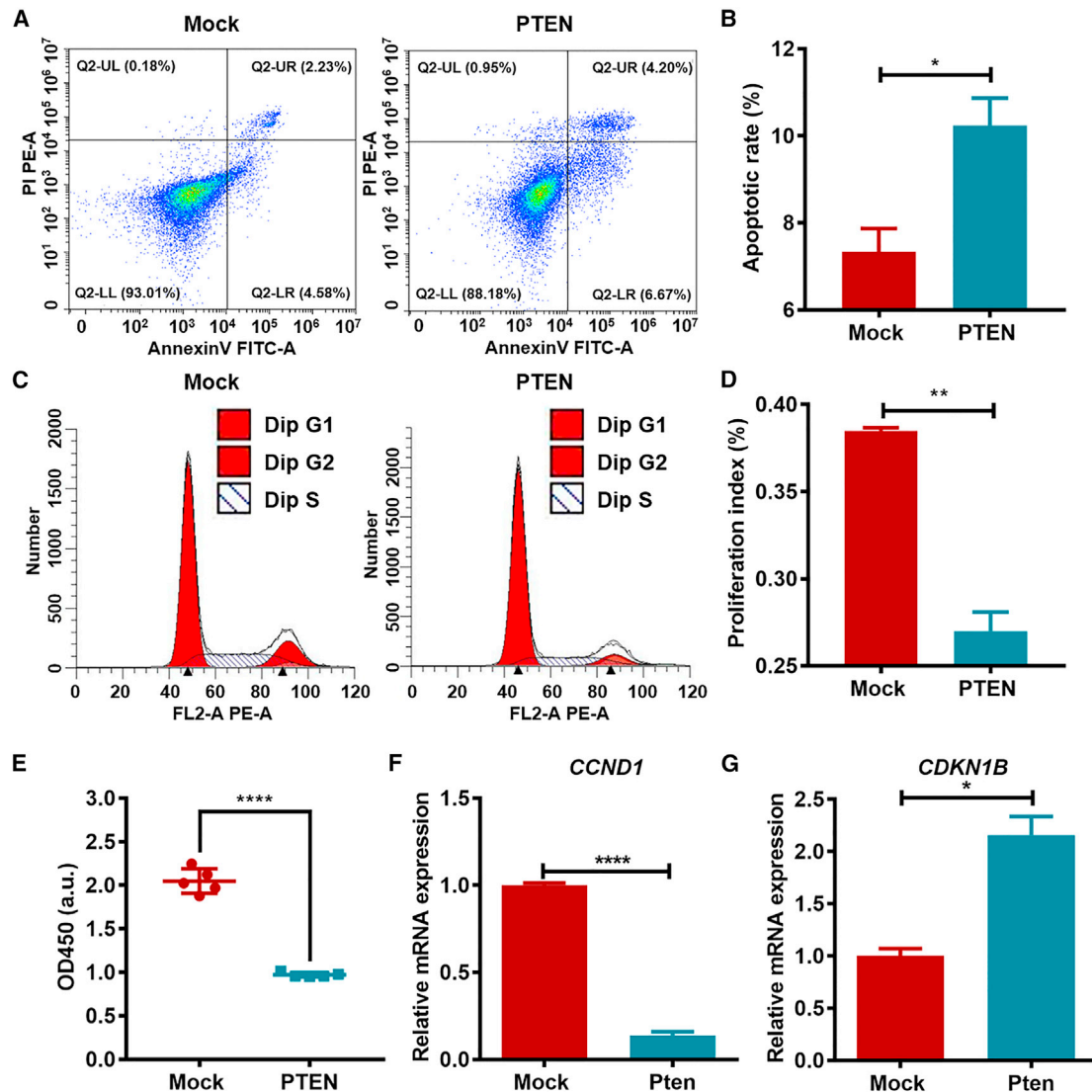


Figure 4. PTEN overexpression significantly promotes cell apoptosis and inhibits the cell cycle by regulating CCND1 and CDKN1B expression

(A and B) PC3 cell apoptosis was detected by flow cytometry. Q2-UR represents (double-positive) late-stage apoptosis, and Q2-LR represents (FITC-positive/PI-negative) early stage apoptosis. (C and D) The cell cycle was analyzed by flow cytometry. The number of cells in the G₂ and S phases in the PTEN group was significantly lower than that in the mock group. (E) The effect of PTEN on PC3 cell proliferation was measured using the CCK-8 assay. (F and G) CCND1 and CDKN1B expression was detected using qPCR. The experiments were performed in triplicate, and representative images of cytometry are presented in (A and C) **p* < 0.05; ***p* < 0.01; *****p* < 0.0001.

CDKN1B have been extensively demonstrated to be deleted or mutated in PCa in cohorts from Western countries and Asian populations. These findings suggest that PCa progression can be significantly inhibited by PTEN and CDKN1B overexpression. In combination with the rAAV vector, genes of interest can be effectively delivered to normal prostate tissue and PCa cells, as previously described. Furthermore, our data showed that PTEN and CDKN1B inhibited tumor cell growth *in vitro* and *in vivo*, which reveals an opportunity for the development of alternative treatments for PCa.

In terms of the suppressive role of PTEN, TCGA data suggest that PTEN deletion or mutation dramatically decreased the survival of PCa patients (data not shown) and that its low expression was stably detected in samples with different Gleason scores and in those with different degrees of lymph node metastasis, which suggests that PTEN might be an ideal target for PCa treatment. Interestingly, the synergistic expression of PTEN and CDKN1B further suggested the potential role of PTEN gene delivery in inhibiting PCa. By regulating CDKN1B and CCND1 expression, PTEN significantly inhibits the cell cycle at G₁ phase and

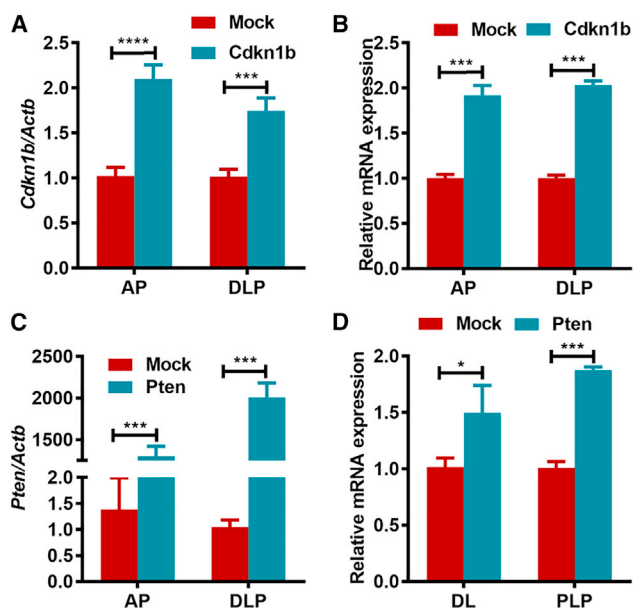


Figure 5. Cdkn1b and Pten DNA and mRNA levels in the AP and DLP after intraprostatic injection

(A and B) DNA and mRNA levels of Cdkn1b were detected using qPCR. (C and D) DNA and mRNA levels of Pten were detected using qPCR. Prostate tissues from 5 mice each were used for DNA and mRNA detection. * $p < 0.05$; *** $p < 0.001$; **** $p < 0.0001$.

promotes both early stage and late-stage apoptosis in PCa cells *in vitro*.

Notably, intraprostatic injection of rAAV9.Pten and rAAV9.Cdkn1b markedly increased the survival rates of TRAMP mice. The median survival time increased from 220 days in the mock group to 301 and 365 days in the Pten and Cdkn1b groups, respectively. The single deletion of CDKN1B did not lead to tumorigenesis; however, the reduction in Cdkn1b gene expression accelerated tumorigenesis in Pten^{+/-} mice.¹⁶ Conversely, the combined delivery of PTEN and CDKN1B might result in a greater therapeutic effect on PCa than single-gene delivery. Consistent with our *in vitro* results, Pten promoted Cdkn1b expression and Ctnnb1 phosphorylation and decreased Ccnd1 expression *in vivo*, which again verifies the mechanism through which PTEN regulates PCa progression. Importantly, CTNNB1 phosphorylation is directly regulated by the PTEN/AKT/GSK3 β signaling pathway; namely, PTEN overexpression activates the GSK3 β function and increases CTNNB1 phosphorylation, and then the phosphorylation of CTNNB1 is degraded by the proteasome.^{29,30} Expression of downstream genes, which promote cell-cycle progression and survival, was decreased, and cancer progression was inhibited.

In our study, rAAVs at a dose of 4×10^{11} gene copies (GC) were administered intraperitoneally and amounted to 1.74×10^{13} GC/kg, given that 8-week-old mice had an average weight of 23 g. Although this dose appears high, a preclinical study in dogs using

semisystemic intraportal administration of rAAV8 reported the safe administration of 4.95×10^{13} GC/kg, which supports the safety and feasibility of our dose.³¹ Particularly, our study included two *in vivo* mouse models to investigate the therapeutic role of PTEN and CDKN1B in PCa. The PCa condition was simulated in the TRAMP model, as mice exhibit various forms of disease from mild intraepithelial hyperplasia to large multinodular malignant neoplasia.³² The TRAMP-C2 xenograft model was established by injecting TRAMP-C2 cells into wild-type C57/B6 mice. These two models were established in mice with normal immune systems; hence, the therapeutic effect of rAAV-based gene delivery, demonstrated by its inhibition of PCa progression, provides strong evidence for its clinical translation and application.

In summary, the expression of PTEN and its downstream gene CDKN1B were significantly reduced in human and mouse PCa samples compared with control samples; when expressed, these genes effectively inhibited PCa progression *in vitro* and *in vivo* by promoting apoptosis and inducing cell-cycle arrest. By utilizing the rAAV-based gene delivery system, rAAV.Pten and rAAV.Cdkn1b showed promising curative effects for PCa. The findings of our study provide an important alternative for clinicians and patients.

MATERIALS AND METHODS

TCGA data analysis

The alteration frequency of PTEN among different studies was obtained from cBioPortal for Cancer Genomics (<http://www.cbioportal.org/>).^{33,34} The gene expression profile and promoter methylation data were obtained from UALCAN (<http://ualcan.path.uab.edu/index.html>)³⁵ and TCGA datasets (<https://portal.gdc.cancer.gov/>). Furthermore, the gene expression data were normalized according to an algorithm of transcripts per kilobase of exon model per million mapped reads (TPM).

Cell culture and TRAMP model

PC3 and TRAMP-C2 cells, which are human and mouse PCa cell lines, respectively, were obtained from ATCC (CRL-1435 and CRL-2731, Manassas, VA, USA). They were cultured in F-12K and DMEM supplemented with 10% fetal bovine serum (FBS) and 1% ampicillin/streptomycin at 37°C in a humidified atmosphere of 5% CO₂. C42B-MDV cells with enzalutamide (#s1250, Selleck, Shanghai, China) resistance were gifted from our collaborator, and these cells were cultured with 1640 Medium containing 20 μ M of enzalutamide. In addition, the TRAMP mice were purchased from Jackson Laboratory and were housed under a 12-h light cycle and a 12-h dark cycle per the requirements of the Institutional Animal Care and Use Committee (IACUC) of the University of Massachusetts Medical School.

Production and titration of rAAV plasmids

The rAAV plasmids used in this study were produced, purified, and titrated by the vector core of the University of Massachusetts Medical School, as previously described.³⁶

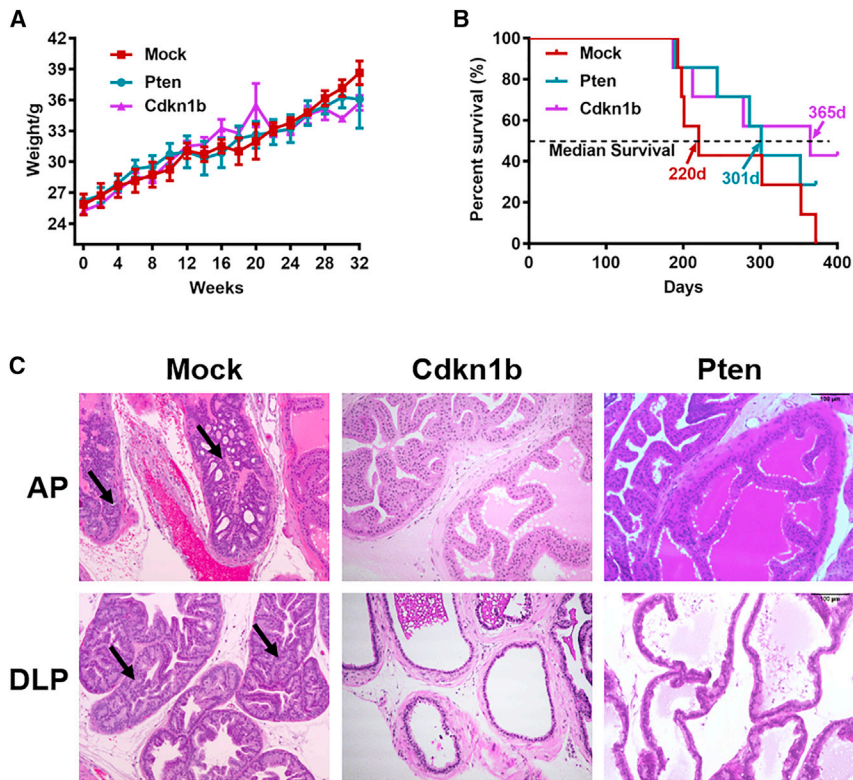


Figure 6. Pten and Cdkn1b improve survival by alleviating neoplasia

(A) The body weights of the mice were recorded every 2 weeks ($n = 7/\text{group}$). (B) The survival of mice was monitored every day, and the median survival is indicated by the arrows ($n = 7/\text{group}$). (C) H&E staining of the AP and DLP illustrates the pathological changes in mouse prostates treated with Cdkn1b and Pten. Areas of neoplasia are indicated by black arrows ($n = 5/\text{group}$). Representative images are presented.

were measured every 3 days. The tumor volume was calculated according to the following formula: $L \times W^2 \times 0.5236$, where L is tumor length and W is tumor width.²¹ Fifteen days later, mice bearing TRAMP-C2 xenografts were sacrificed, after which tumor tissues were harvested and H&E staining and a terminal deoxynucleotidyl transferase (TdT)-mediated dUTP nick end labeling (TUNEL) assay were performed.

Quantitative polymerase chain reaction (qPCR)

First, total RNA was extracted using an AllPrep DNA/RNA Mini Kit from QIAGEN (80,204, Germantown, MD, USA), and cDNA was synthesized using a High-Capacity cDNA Reverse Transcription Kit from Thermo Fisher (4368814, Thermo Fisher Scientific, Waltham, MA, USA). Second, qPCR was performed under the following reaction conditions: one cycle at 95°C for 2 min and 40 cycles at 95°C for 5 s and 60°C for 10 s. The relative mRNA expression was determined using the $2^{-\Delta\Delta t}$ method. Beta-actin served as an internal control, and all experiments were performed in triplicate.

Western blotting

Total proteins were harvested using a radio-immunoprecipitation assay (RIPA) lysis buffer. Briefly, proteins were separated by 10% SDS-PAGE and transferred onto a polyvinylidene fluoride (PVDF) membrane at 220 mA for 90 min. After blocking with 5% skimmed milk, the membranes were incubated with the primary antibodies at 4°C overnight. Next, the membranes were incubated with secondary antibodies at room temperature (RT) for 1 h. Finally, the protein bands were developed using an enhanced chemiluminescence (ECL) kit. Additionally, primary antibodies against Pten (Cat. No. ab267787), Cnd1 (Cat. No. ab134175), Cdkn1b (Cat. No. ab193379), Actb (Cat. No. ab6276), and p-Ctnnb (cat. no. ab27798), as well as goat anti-rabbit immunoglobulin G (IgG) H&L (HRP) (Cat. No. ab6721) and goat anti-mouse IgG H&L (horseradish peroxidase [HRP]) (Cat. No. ab6789) secondary antibodies were purchased from Abcam (Cambridge, MA, USA). The intensities of the protein bands were evaluated using ImageJ software, and all experiments were performed in triplicate.

Lentivirus production

Briefly, 293T cells were seeded into a 6-well plate for 16–24 h, and then cells were cultured with medium containing $25 \mu\text{M}$ of chloroquine. Next, $100 \mu\text{L}$ of mixture containing $2 \mu\text{g}$ of psPAX2 (Addgene #12260), $1 \mu\text{g}$ of pMD2.G (Addgene #12259), $4 \mu\text{g}$ of *cis*-plasmid-expressing PTEN or CDKN1B, and $12.5 \mu\text{L}$ of 2M CaCl_2 was added with $2\times\text{HBS}$ solution using a vortex. Then, the mixture was slowly added into the culture medium. The culture medium was replaced after 12 h of transfection, and the supernatant was harvested after 36, 48, and 60 h of co-transfection. Finally, the lentiviral crude lysate was filtrated using a $0.45 \mu\text{m}$ filter.

Animal studies

Eight-week-old male TRAMP mice were used in this study, and 4×10^{11} GC of rAAV9.Pten or rAAV9.Cdkn1b plasmids in $40 \mu\text{L}$ of phosphate-buffered saline (PBS) were intraprostatically injected into two lobes of the AP and DLP ($n = 7/\text{group}$). The body weight of the mice was recorded every other week, and the survival status was observed daily. In addition, the mouse prostates were harvested for gene expression detection and histopathology 4 weeks after viral injection ($n = 5/\text{group}$). TRAMP-C2 cells were cultured as described above. In total, 3×10^6 cells were injected into the right flank of male C57/B6 mice. The tumor volume reached approximately 100mm^3 7–8 weeks after subcutaneous injection. Subsequently, 5×10^{11} GC rAAV particles were injected into the tumor at a single site. The length and width of the tumor

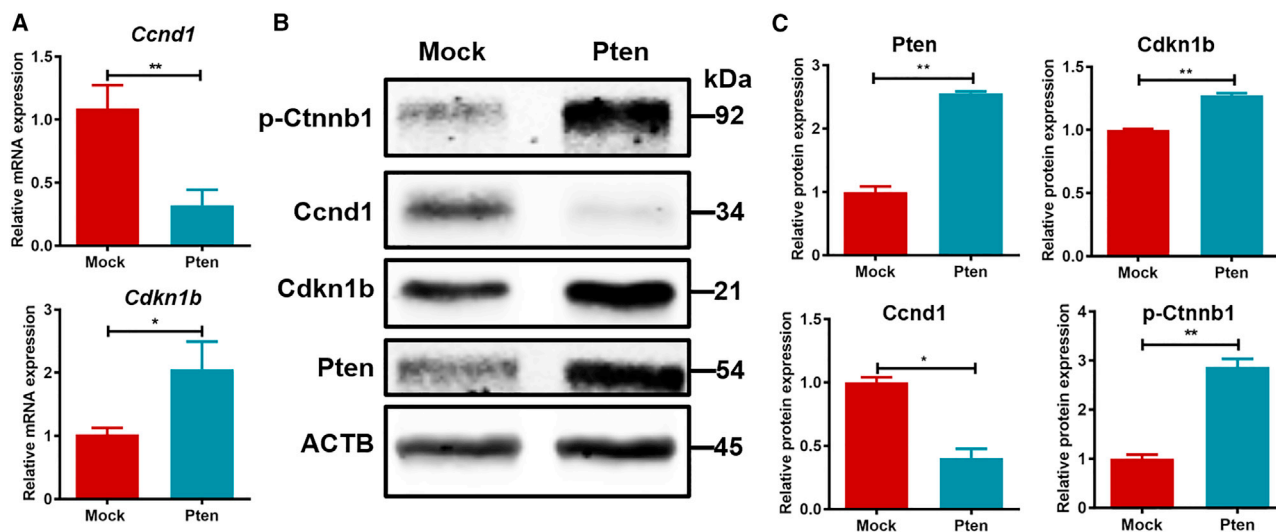


Figure 7. Pten regulates downstream gene expression

(A) qPCR detection of *Ccnd1* and *Cdkn1b* in mouse prostate tissues ($n = 5/\text{group}$). (B) The expression of phosphorylated *Ccnd1*, *Cdkn1b*, *Pten*, and *Ctnnb1* was detected by western blotting, and representative images of protein bands from one animal each are shown. (C) The protein bands as shown in (B) from 5 animals each were quantitated using ImageJ software. * $p < 0.05$; ** $p < 0.01$.

Wound-healing assay

Cell migration was assessed *in vitro* using a wound-healing assay. In all, 3×10^5 cells were seeded into a 6-well plate, after which the cells were transfected with a *PTEN* overexpression plasmid for 48 h. Then, the cell monolayer was scratched with a 10 μL tip, and the wound widths were recorded after 0, 24, 48, and 72 h of transfection. The wound width was measured using ImageJ software, and all experiments were performed in triplicate.

Cell apoptosis analysis

Cell apoptosis was analyzed using a kit purchased from KeyGEN BioTECH (KGA108-2, Nanjing, China). After 48 h of transfection or infection, PC3 or C42B-MDV cells in a 6-well plate were digested with trypsin without EDTA, and the cells were washed twice in PBS for 5 min. Next, cells were suspended in 500 μL of binding buffer and incubated with 5 μL of annexin V-fluorescein isothiocyanate (FITC) and 5 μL of propidium iodide for 15 min. Apoptosis rates were determined using a CytoFLEX flow cytometer (Beckman Coulter, Brea, CA, USA), and all experiments were performed in triplicate.

Cell-cycle detection

The cell cycle was analyzed using a kit from KeyGEN BioTECH (KGA512, Nanjing, China). Cells transfected with plasmids or infected with lentiviruses for 48 h were harvested by digestion and centrifugation at 400 g for 5 min, after which the cells were fixed overnight in 70% pre-cooled ethanol. Fixed cells were centrifuged at 400 g for 3 min and incubated with 500 μL of propidium iodide/RNase A mixture (9:1, v/v); the cell-cycle status was detected using a CytoFLEX flow cytometer (Beckman Coulter, Brea, CA, USA). The proliferation index was calculated as follows: proliferation index (PI) = $(S + G_2/M)/(G_0/1 + S + G_2/M) \times 100\%$, and all experiments were performed in triplicate.

Cell viability assay

A CCK-8 purchased from Dojindo was used to evaluate cell proliferation. After transfection with the *PTEN* plasmid for 48 h, 10 μL of the CCK-8 solution was added to each well of a 96-well plate, and the plate was further incubated at 37°C for 2 h. Furthermore, the optical density at 450 nm was measured using a microplate reader, and all experiments were performed in triplicate.

H&E staining

Histological analysis was performed as previously described.¹⁸ Briefly, tissues were fixed in 4% paraformaldehyde overnight at RT, embedded in paraffin, and sectioned at a 4 μm thickness. The sections were stained with H&E and imaged under a microscope (Leica, Buffalo Grove, IL, USA).¹⁸

TUNEL assay

PCa cell apoptosis was assessed using the DeadEnd Colorimetric TUNEL System from Promega (G7360, Madison, WI, USA). Briefly, the slides were deparaffinized in two changes of xylene (5 min each), and the slides were rehydrated in decreasing concentrations of ethanol (100%, 95%, 85%, 70%, and 50%) for 3 min each time. After the slides were fixed in 4% paraformaldehyde in PBS for 15 min, tissues were treated with 100 μL of a 20 $\mu\text{g}/\text{mL}$ Proteinase K solution at RT for 30 min and refixed in 4% paraformaldehyde in PBS for 5 min. Next, slides were equilibrated using 100 μL of equilibration buffer at RT for 10 min and then incubated with 100 μL of TdT reaction mixture for 1 h at 37°C in a humidified chamber. Then, the reaction was stopped using $2 \times$ saline sodium citrate (SSC) for 15 min, after which the slides were blocked in 0.3% hydrogen peroxide for 5 min. Furthermore, the slides were incubated with 100 μL of streptavidin HRP (diluted 1:500 in PBS) for 30 min at RT and stained with 100 μL of diaminobenzidine

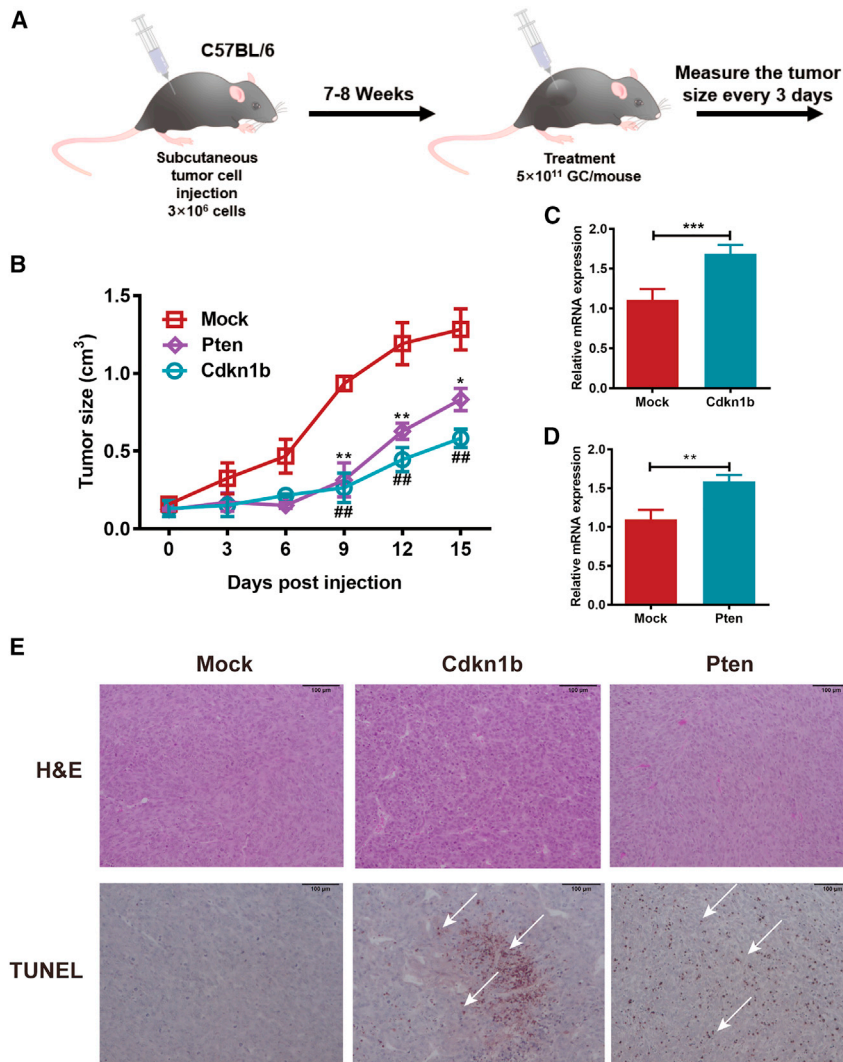


Figure 8. Pten and Cdkn1b significantly inhibits tumor growth in a subcutaneous xenograft model

(A) A schematic diagram illustrates the establishment of the xenograft model and intratumoral injection of rAAV.Pten or rAAV.Cdkn1b. (B) The tumor volume was measured every 3 days. Significant differences among these groups were observed 9 days after injection. (C) Cdkn1b and Pten expression in xenografts was detected using qPCR. (E) H&E staining shows the pathological status of xenograft tumors, and a TUNEL assay was used to evaluate tumor cell apoptosis, as indicated by the white arrow. Representative images of the TUNEL assay are shown ($n = 4/\text{group}$). * $p < 0.05$; ** $p < 0.01$; *** $p < 0.001$.

(DAB) solution until a light brown background appeared. Finally, staining was visualized by light microscopy after several washes.

Statistical analysis

All data are presented as means \pm standard error of the mean (SEM) or standard deviation (SD). The statistical significance of comparisons among multiple groups (>3) and between groups was determined using analysis of variance (ANOVA) and Student's paired t test, respectively, in GraphPad Prism 7.0. The statistical analyses were performed on the survival using log rank test. A p value < 0.05 was considered significant.

SUPPLEMENTAL INFORMATION

Supplemental information can be found online at <https://doi.org/10.1016/j.omtn.2021.11.018>.

ACKNOWLEDGMENTS

We thank Drs. Shiyu Zhang, Hang Xu, and Dazhou Liao for assisting the revision. We also thank Dr. Bo Chen for the gift of C42B-MDV cell line and Dr. Liyuan Xiang from the Clinical Research Management Department of West China Hospital of Sichuan University for the TCGA data mining. This study was supported by grants from the National Natural Science Foundation of China (82070784 and 81702536) and Science & Technology Department of Sichuan Province, China (22CXRC0166) to J.A.; grants from the University of Massachusetts Medical School (an internal grant) and National Institutes of Health (R01NS076991-01, 1P01AI100263-01, UG3 HL147367-01, 4P01HL131471-02, and R01HL097088) to G.G.; and a grant from 1.3.5 project for disciplines of excellence, West China Hospital, Sichuan University (ZYG18011) to H.L.

AUTHOR CONTRIBUTIONS

J.A. and G.G. conceived the project and drafted the manuscript, J.A., J.L., Q.S., and H.M. conducted experiments and analyzed data, and Q.W. and H.L. revised the manuscript.

DECLARATION OF INTERESTS

G.G. is a co-founder of Voyager, Adrenas, and AspA Therapeutics, specialized in rAAV-based gene therapy, and holds equity in the companies. G.G. is an inventor on patents with potential royalties licensed to Voyager, AspA, and other biopharmaceutical companies.

REFERENCES

- Bray, F., Ferlay, J., Soerjomataram, I., Siegel, R.L., Torre, L.A., and Jemal, A. (2018). Global cancer statistics 2018: GLOBOCAN estimates of incidence and mortality worldwide for 36 cancers in 185 countries. *CA Cancer J. Clin.* 68, 394–424.
- Olson, B.M., and McNeel, D.G. (2011). Sipuleucel-T: immunotherapy for advanced prostate cancer. *Open Access J. Urol.* 3, 49–60.
- de Bono, J.S., Logothetis, C.J., Molina, A., Fizazi, K., North, S., Chu, L., Chi, K.N., Jones, R.J., Goodman, O.B., Jr., Saad, F., et al. (2011). Abiraterone and increased survival in metastatic prostate cancer. *N. Engl. J. Med.* 364, 1995–2005.
- Scher, H.I., Fizazi, K., Saad, F., Taplin, M.E., Sternberg, C.N., Miller, K., de Wit, R., Mulders, P., Chi, K.N., Shore, N.D., et al. (2012). Increased survival with enzalutamide in prostate cancer after chemotherapy. *N. Engl. J. Med.* 367, 1187–1197.
- Barata, P.C., and Sartor, A.O. (2019). Metastatic castration-sensitive prostate cancer: abiraterone, docetaxel, or. *Cancer* 125, 1777–1788.
- Muhammad, L.A., and Saad, F. (2015). The role of clusterin in prostate cancer: treatment resistance and potential as a therapeutic target. *Expert Rev. Anticancer Ther.* 15, 1049–1061.
- Vaillant, O., El Cheikh, K., Warther, D., Brevet, D., Maynadier, M., Bouffard, E., Salgues, F., Jeanjean, A., Puche, P., Mazerolles, C., et al. (2015). Mannose-6-phosphate receptor: a target for theranostics of prostate cancer. *Angew. Chem. Int. Ed. Engl.* 54, 5952–5956.
- Wu, H., You, L., Li, Y., Zhao, Z., Shi, G., Chen, Z., Wang, Z., Li, X., Du, S., Ye, W., et al. (2020). Loss of a negative feedback loop between IRF8 and AR promotes prostate cancer growth and enzalutamide resistance. *Cancer Res.* 80, 2927–2939.
- Braglia, L., Zavatti, M., Vinceti, M., Martelli, A.M., and Marmiroli, S. (2020). Deregulated PTEN/PI3K/AKT/mTOR signaling in prostate cancer: still a potential druggable target? *Biochim. Biophys. Acta Mol. Cell Res.* 1867, 118731.
- Akula, S.M., Abrams, S.L., Steelman, L.S., Emma, M.R., Augello, G., Cusimano, A., Azzolina, A., Montalto, G., Cervello, M., and McCubrey, J.A. (2019). RAS/RAF/MEK/ERK, PI3K/PTEN/AKT/mTORC1 and TP53 pathways and regulatory miRs as therapeutic targets in hepatocellular carcinoma. *Expert Opin. Ther. Targets* 23, 915–929.
- Carbognin, L., Miglietta, F., Paris, I., and Dieci, M.V. (2019). Prognostic and predictive implications of PTEN in breast cancer: unfulfilled promises but intriguing perspectives. *Cancers (Basel)* 11, 1401.
- Gkountakos, A., Sartori, G., Falcone, I., Piro, G., Ciuffreda, L., Carbone, C., Tortora, G., Scarpa, A., Bria, E., Milella, M., et al. (2019). PTEN in lung cancer: dealing with the problem, building on new knowledge and turning the game around. *Cancers (Basel)* 11, 1141.
- Salvatore, L., Calegari, M.A., Loupakis, F., Fassan, M., Di Stefano, B., Bensi, M., Bria, E., and Tortora, G. (2019). PTEN in colorectal cancer: shedding light on its role as predictor and target. *Cancers (Basel)* 11, 1765.
- Zhao, D., Cai, L., Lu, X., Liang, X., Li, J., Chen, P., Ittmann, M., Shang, X., Jiang, S., Li, H., et al. (2020). Chromatin regulator, CHD1, remodels the immunosuppressive tumor microenvironment in PTEN-deficient prostate cancer. *Cancer Discov.* 10, 1374–1387.
- Li, J., Xu, C., Lee, H.J., Ren, S., Zi, X., Zhang, Z., Wang, H., Yu, Y., Yang, C., Gao, X., et al. (2020). A genomic and epigenomic atlas of prostate cancer in Asian populations. *Nature* 580, 93–99.
- Di Cristofano, A., De Acetis, M., Koff, A., Cordon-Cardo, C., and Pandolfi, P.P. (2001). Pten and p27KIP1 cooperate in prostate cancer tumor suppression in the mouse. *Nat. Genet.* 27, 222–224.
- Radu, A., Neubauer, V., Akagi, T., Hanafusa, H., and Georgescu, M.M. (2003). PTEN induces cell cycle arrest by decreasing the level and nuclear localization of cyclin D1. *Mol. Cell Biol.* 23, 6139–6149.
- Ai, J., Li, J., Gessler, D.J., Su, Q., Wei, Q., Li, H., and Gao, G. (2017). Adeno-associated virus serotype rh.10 displays strong muscle tropism following intraperitoneal delivery. *Sci. Rep.* 7, 40336.
- Ai, J., Wang, D., Wei, Q., Li, H., and Gao, G. (2016). Adeno-associated virus serotype vectors efficiently transduce normal prostate tissue and prostate cancer cells. *Eur. Urol.* 69, 179–181.
- Ai, J., Tai, P.W.L., Lu, Y., Li, J., Ma, H., Su, Q., Wei, Q., Li, H., and Gao, G. (2017). Characterization of adenoviral transduction profile in prostate cancer cells and normal prostate tissue. *Prostate* 77, 1265–1270.
- Watanabe, M., Nasu, Y., Kashiwakura, Y., Kusumi, N., Tamayose, K., Nagai, A., Sasano, T., Shimada, T., Daida, H., and Kumon, H. (2005). Adeno-associated virus 2-mediated intratumoral prostate cancer gene therapy: long-term maspin expression efficiently suppresses tumor growth. *Hum. Gene Ther.* 16, 699–710.
- Ai, J., Li, J., Su, Q., Ma, H., He, R., Wei, Q., et al. (2021). rAAV-based and intraprostatically delivered miR-34a therapeutics for efficient inhibition of prostate cancer progression. *Gene Ther.* <https://doi.org/10.1038/s41434-021-00275-5>.
- Moradi, A., Srinivasan, S., Clements, J., and Batra, J. (2019). Beyond the biomarker role: prostate-specific antigen (PSA) in the prostate cancer microenvironment. *Cancer Metastasis Rev.* 38, 333–346.
- Tan, M.H., Li, J., Xu, H.E., Melcher, K., and Yong, E.L. (2015). Androgen receptor: structure, role in prostate cancer and drug discovery. *Acta Pharmacol. Sin.* 36, 3–23.
- Penning, T.M. (2015). Mechanisms of drug resistance that target the androgen axis in castration resistant prostate cancer (CRPC). *J. Steroid Biochem. Mol. Biol.* 153, 105–113.
- Thoma, C. (2016). Prostate cancer: interfering with abiraterone metabolism to optimize therapy. *Nat. Rev. Urol.* 13, 370.
- Scott, L.J. (2018). Enzalutamide: a review in castration-resistant prostate cancer. *Drugs* 78, 1913–1924.
- Attard, G., and Antonarakis, E.S. (2016). Prostate cancer: AR aberrations and resistance to abiraterone or enzalutamide. *Nat. Rev. Urol.* 13, 697–698.
- Zhang, R., Li, G., Zhang, Q., Tang, Q., Huang, J., Hu, C., Liu, Y., Wang, Q., Liu, W., Gao, N., et al. (2018). Hirsutine induces mPTP-dependent apoptosis through ROCK1/PTEN/PI3K/GSK3beta pathway in human lung cancer cells. *Cell Death Dis.* 9, 598.
- Shen, H., Li, L., Yang, S., Wang, D., Zhong, S., Zhao, J., and Tang, J. (2016). MicroRNA-29a contributes to drug-resistance of breast cancer cells to adriamycin through PTEN/AKT/GSK3beta signaling pathway. *Gene* 593, 84–90.
- Marcos-Contreras, O.A., Smith, S.M., Bellinger, D.A., Raymer, R.A., Merricks, E., Faella, A., Pavani, G., Zhou, S., Nichols, T.C., High, K.A., et al. (2016). Sustained correction of FVII deficiency in dogs using AAV-mediated expression of zymogen FVII. *Blood* 127, 565–571.
- Kido, L.A., de Almeida Lamas, C., Marostica, M.R., Jr., and Cagnon, V.H.A. (2019). Transgenic Adenocarcinoma of the Mouse Prostate (TRAMP) model: a good alternative to study PCa progression and chemoprevention approaches. *Life Sci.* 217, 141–147.
- Cerami, E., Gao, J., Dogrusoz, U., Gross, B.E., Sumer, S.O., Aksoy, B.A., Jacobsen, A., Byrne, C.J., Heuer, M.L., Larsson, E., et al. (2012). The cBio cancer genomics portal: an open platform for exploring multidimensional cancer genomics data. *Cancer Discov.* 2, 401–404.
- Gao, J., Aksoy, B.A., Dogrusoz, U., Dresdner, G., Gross, B., Sumer, S.O., Sun, Y., Jacobsen, A., Sinha, R., Larsson, E., et al. (2013). Integrative analysis of

- complex cancer genomics and clinical profiles using the cBioPortal. *Sci. Signal.* 6, p11.
35. Chandrashekar, D.S., Bashel, B., Balasubramanya, S.A.H., Creighton, C.J., Ponce-Rodriguez, I., Chakravarthi, B., and Varambally, S. (2017). UALCAN: a portal for facilitating tumor subgroup gene expression and survival analyses. *Neoplasia* 19, 649–658.
36. Su, Q., Sena-Esteves, M., and Gao, G. (2020). Production of recombinant adeno-associated viruses (rAAVs) by transient transfection. *Cold Spring Harb. Protoc.* 2020, 095596.